Effect of Two Typical Wing Forms on Aerodynamic Characteristics of Double-ellipsoidal Airship

Yuan Liu [1], Hu Ye [1], Yunfei Li [1], Xiaolong Wu [1], Du Lu [1], Xuan Yao [1], Taiqin Huang [1]

[1] *Northwestern Institution of Nuclear Technology, No.85, Lintong District, Xi'an, China*

Abstract

Aiming at the problem that the effect of two-typical wing forms on aerodynamic characteristics of double-ellipsoidal airship, the aerodynamic characteristics of airship with X-shaped tail and inverted Y-shaped tail are studied respectively. Based on the method of Computational Fluid Dynamics (CFD), the aerodynamic characteristics of airships with the same hull shape parameters are simulated, at an angle of attack ranging from -30 to 30 degrees and angle of sideslip ranging from 0 to 20 degree. The result shows that the double-ellipsoidal airship with inverted Y-shaped tail has a certain advantage in reducing hull resistance, compared with the airship with X-shaped tail. The double-ellipsoidal airship with X-shaped tail has better ability to provide lift force and maintain hull stability, compared with the airship with inverted Y-shaped tail. The simulation results provide an effective reference for aerodynamic shape design and flight control strategy of double-ellipsoidal airship.

Keywords

Airship, CFD, Aerodynamic characteristics, Numerical simulation

1. Introduction

Airship is a kind of aircraft which can fly by air buoyancy and propulsion system [1]. Airship can stay in the air for a long time with the low cost of manufacturing and flying, and it has good concealment performance and a large payload. Airship is widely used in communication relay, early warning detection, electronic countermeasures, intelligence investigation and other fields. The airship is in a changing atmospheric environment under cruise and dwell conditions. In the overall design of airship, aerodynamic characteristics are a crucial link, which affects the handling performance and working state of airship [2]. The tail wing of airship is a part of the hull subsystem, which is generally installed at the rear of the hull. The tail wing plays a role of stable balance in flight control and has a great influence on the overall aerodynamic characteristics of airship. The layout of airship tail mainly includes X-shaped tail, Y-shaped tail, inverted Y-shaped tail and cross shaped tail. In the development history of airship, all countries have carried out different degrees of research on the aerodynamic characteristics of airship.

Aiming at the influence of tail airfoil on tethered balloons, Zhang Guifu [3] simulated and analyzed tethered balloons with four different tail airfoils, and the effects of airfoil thickness and airfoil curvature on the lift, drag and pitching moment of tethered balloon are discussed. Zhang Haijun [4] applied the LES method to calculate the flow field around the airship under the condition of 0 degrees angle of attack, and made a comparative analysis of LOTTE airship and M-LOTTE airship. Zhang Dan [5] used realizable k-ε turbulence model to simulate the separated flow and vortex structure of biaxial ellipsoid airship at different angles of attack. Jin Anfan and Song Wenping [6] used the Reynolds average N-S equation as the governing equation and the finite volume method to construct the spatial discrete scheme, and the resistance characteristics of different hull shapes are calculated, and the best hull shape is obtained. Wang Xiaoliang [7] used the aerodynamic engineering calculation method combining the

ISCIPT2022@7th International Conference on Computer and Information Processing Technology, August 5-7, 2022, Shenyang, China
EMAIL: laurelyard@qq.com (Yuan Liu); 1679375887@qq.com (Hu Ye); laurelyard@qq.com (Yunfei Li); laurelyard@qq.com (Xiaolong Wu); laurelyard@qq.com (Du Lu); laurelyard@qq.com (Xuan Yao); laurelyard@qq.com (Taiqin Huang);

finite basic solution and engineering estimation method to calculate the aerodynamic force on the airship hull and tail respectively, according to the linear aerodynamic force generated by inviscid fluid and the nonlinear aerodynamic force caused by viscosity. Lin Ruikun [8] used realizable k-ε turbulence model to simulate the tail vortex structure of airship with propeller at high angle of attack. Li Tiane [9] took an airship with a cylindrical section in the middle as the research object. On the basis of verifying the numerical simulation method, Li analyzed the effects of tail, slenderness ratio, height and Reynolds number on the aerodynamic resistance of airship. With the goal of reducing aerodynamic resistance and improving the maneuverability of airship, Wang Weizhi [10] used CFD method to find the optimal combination of hull, pod and tail wing. The above literature mainly analyzes the aerodynamic characteristics of airships under different flow fields, but there is still a lack of in-depth research on the aerodynamic characteristics of airships with different tail forms.

2. Numerical calculation model

The Reynolds number of the flow field studied in this paper is in the order of 10^7, so the turbulence model is used. The main function of turbulence model is to connect the new unknowns with the average velocity gradient. The standard model id based on the model of two transport equations to solve *k* and *ε*. The coefficient is given by empirical formula, which has many applications, moderate calculation amount and more data accumulation. Convergence and calculation accuracy can meet the general engineering calculation requirements [11]. In this paper, the standard *k*-*ε* model is used as the turbulence model of airship aerodynamic characteristics simulation, which is an incompressible/compressible two equation eddy viscosity model integrated to the wall.

The eddy viscosity model of Reynolds stress is [12]

$$\tau_{tij} = -\rho\overline{u}u_j = 2\mu_t(S_{ij} - S_{nm}\delta_{ij}/3) - 2\rho k\delta_{ij}/3 \tag{1}$$

Where μ_t is the eddy viscosity and S_{ij} is the mean-velocity strain-rate tensor, ρ is the fluid density, *k* is the turbulent kinetic energy, and δ_{ij} is the Kronecker delta. Eddy viscosity is defined as a function of turbulent kinetic energy *k* and turbulent dissipation rate ε.

$$\mu_t = C_\mu f_\mu \rho k^2 / \varepsilon \tag{2}$$

Based on dimensional analysis, eddy viscosity is scaled by fluid density ρ, turbulent velocity scale k^2 and length scale $k^{3/2}/\varepsilon$. The attenuation function f is modeled by turbulent Reynolds number $Re_t = \rho k^2/(\varepsilon\mu)$. The turbulent transport equation can be expressed as turbulent energy transport equation (3) and energy dissipation transport equation (4).

$$\frac{\partial(\rho k)}{\partial t} + \frac{\partial}{\partial x_j}(\rho u_j \frac{\partial k}{\partial x_i} - (\mu + \frac{\mu_t}{\sigma_k})\frac{\partial k}{\partial x_j}) = \tau_{tij}S_{ij} - \rho\varepsilon + \phi_k \tag{3}$$

$$\frac{\partial(\rho\varepsilon)}{\partial t} + \frac{\partial}{\partial x_j}(\rho u_j \varepsilon - (\mu + \frac{\mu_t}{\sigma_\varepsilon})\frac{\partial \varepsilon}{\partial x_j}) = c_{\varepsilon 1}\frac{\varepsilon}{k}\tau_{tij}S_{ij} - c_{\varepsilon 2}f_2\rho\frac{\varepsilon^2}{k} + \phi_\varepsilon \tag{4}$$

The right end term represents the production term, dissipation term and wall term respectively.

The values of the constants in the mode are as follows.

$$C_\mu = 0.09 \quad c_{\varepsilon 1} = 1.45 \quad c_{\varepsilon 2} = 1.92$$

$$\sigma_k = 1.0 \quad \sigma_\varepsilon = 1.3 \quad \mathrm{Pr}_t = 0.9$$

The near wall attenuation function is

$$f_\mu = \exp(-3.4/(1+0.02Re_t)^2) \tag{5}$$

$$f_2 = 1 - 0.3\exp(-Re_t^2) \tag{6}$$

$$Re_t = \frac{\rho k^2}{\mu \varepsilon} \tag{7}$$

The wall term is

$$\phi_k = 2\mu(\frac{\partial \sqrt{k}}{\partial y})^2 \tag{8}$$

$$\phi_\varepsilon = 2\mu \frac{\mu_t}{\rho}(\frac{\partial^2 u_s}{\partial y^2})^2 \tag{9}$$

Where u_s is the flow velocity parallel to the wall. The slip free boundary condition integrated to the wall is k=0 and ε =0.

3. Aerodynamic characteristic simulation

For complex flow problems, the numerical simulation method has the advantages of low cost, short time-consuming and easy to obtain the data in the flow field. In this paper, the double ellipsoid hulls with X-shaped tail and inverted Y-shaped tail are numerically simulated by CFD flow simulation software ANSYS FLUENT, and the flow characteristics under different angles of attack and sideslip are analyzed.

3.1. Establish simulation model

The simulation models of double-ellipsoidal airship with X-shaped tail and inverted Y-shaped tail are established respectively. As shown in Figure 1 and Figure 2, the length of the hulls is 100 m and the slenderness ratio is 4. NACA0018 airfoil with relatively large thickness is selected for the tail wings. The trailing edge of the airfoil is the tangent circle of the airfoil curve at about 95% of the theoretical chord length. The chord length of the tail wing tip is 9.4 m, the sweep angle of the leading edge is 1 degree, the span height is 10.4 m, and the trailing edge of the wing root is 8.4 m from the tail of the airship.

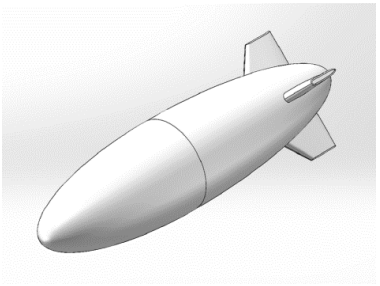

Figure 1: Simulation model of X-shaped airship

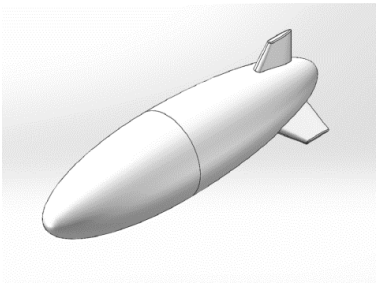

Figure 2: Simulation model of inverted Y-shaped airship

According to the overall dimension of airship, the spatial scale of flow field calculation domain is set as 1000 m × Φ 250 m, so that the flow can be fully developed. Tetrahedral can mesh complex geometric models quickly and efficiently. Tetrahedral mesh is used to topology the computational

domain, and prismatic mesh is added near the wall. It can produce continuous character points in the transition zone. Take the front end of the airship as the origin, and establish the Cartesian coordinate system as shown in the Figure 3.

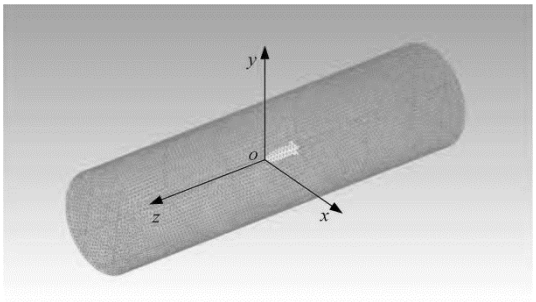

Figure 3: Computational domain grid

The numerical calculation condition is: the airspeed is set to 6m/s, the angle of attack is -30 to 30 degrees and the sideslip angle is 0 to 20 degrees, and the variation of drag coefficient, lift coefficient and pitching moment coefficient is studied.

3.2. Drag coefficient

The drag coefficient is the ratio of the drag on an object to the product of the air pressure and the reference area. When the angle of attack α changes in the range of -30 degrees to 30 degrees, the change of drag coefficient of double-ellipsoidal airships with X-shaped tail, inverted Y-shaped tail and without tail are shown in Figure 4. When the sideslip angle β changes in the range of 0 degrees to 20 degrees, the change of drag coefficient of double-ellipsoidal airships with X-shaped tail, inverted Y-shaped tail and without tail are shown in Figure 5.

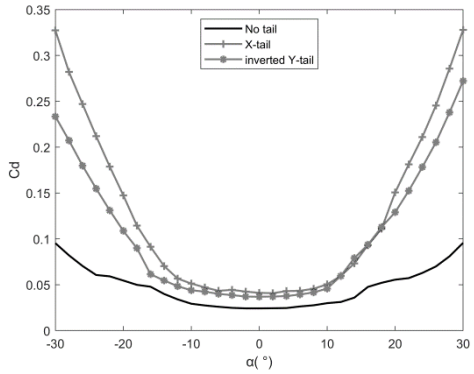

Figure 4: Angle of attack- drag coefficient curve

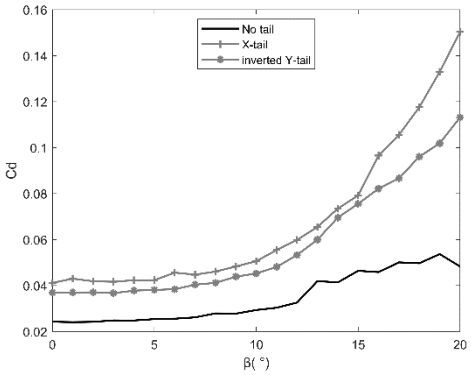

Figure 5: Sideslip angle- drag coefficient curve

The simulation results shows that the existence of tail wing will increase the resistance of double-ellipsoidal airship in flight. The double-ellipsoidal airships with X-shaped tail produces a greater drag coefficient than with inverted Y-shaped tail. With the increase of the angle of attack, this phenomenon is more obvious. When -10 degrees≤α≤10 degrees, the resistance coefficient of airships with X-shaped

tail and inverted Y-shaped tail are about 0.05. When the angle of attack exceeds this range, the drag coefficient will increase significantly. When 0 degrees≤β≤10 degrees, the drag coefficient of airships with X-shaped tail and inverted Y-shaped tail increase at a lower rate. When β≥10 degrees, the growth rate of drag coefficient increases gradually.

3.3. Lift coefficient

The lift coefficient is the ratio of the lift force on an object to the product of the aerodynamic pressure and the reference area. When the angle of attack α changes in the range of -30 degrees to 30 degrees, the change of lift coefficient of double-ellipsoidal airships with X-shaped tail, inverted Y-shaped tail and without tail are shown in Figure 6. When the sideslip angle β changes in the range of 0 degrees to 20 degrees, the change of lift coefficient of double-ellipsoidal airships with X-shaped tail, inverted Y-shaped tail and without tail are shown in Figure 7.

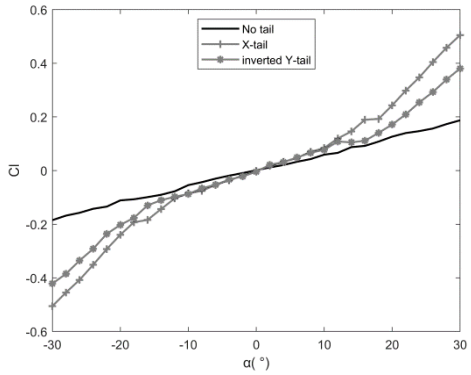

Figure 6: Angle of attack- lift coefficient curve

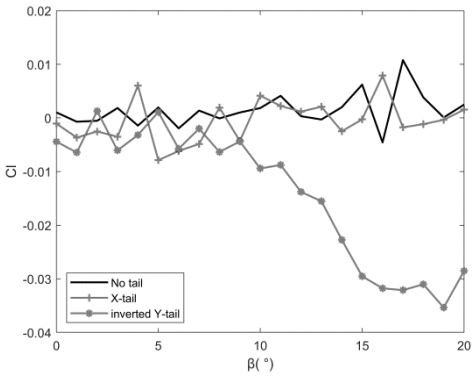

Figure 7: Sideslip angle- lift coefficient curve

The simulation results show that the lift coefficient of double-ellipsoidal airship is mainly a positive correlation trend with the change of angle of attack. When α>0 degrees, the lift coefficient of airship increases gradually. When α<0 degrees, the lift drag coefficient of airship increases gradually. When α>10 degrees, airship with X-shaped tail has a larger lift coefficient than airship with inverted Y-shaped tail. When α<-10 degrees, airship with X-shaped tail has a larger lift drag coefficient than airship with inverted Y-shaped tail. When 0 degrees≤β≤10 degrees, the lift coefficient fluctuates at 0 degrees. When β>10 degrees, compared with airship with X-shaped tail, the lift drag coefficient of airship with inverted Y-shaped tail increases at a faster rate.

3.4. Pitching moment coefficient

The pitching moment coefficient is ratio of the pitching moment received by the object to the product of aerodynamic pressure, reference area and average aerodynamic chord length. When the angle of attack α changes in the range of -30 degrees to 30 degrees, the change of pitching moment coefficient

of double-ellipsoidal airships with X-shaped tail, inverted Y-shaped tail and without tail are shown in Figure 8. When the angle of attack α changes in the range of 0 degrees to 30 degrees, the pitching moment comparison of hull and tail wing of double-ellipsoidal airship is shown in Figure 9.

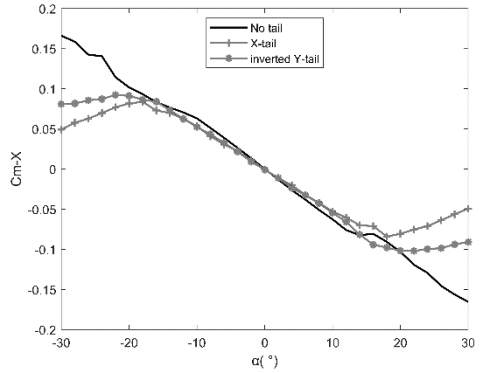

Figure 8: Angle of attack- pitching moment coefficient curve

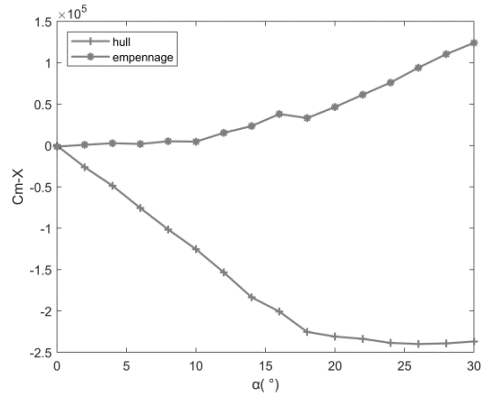

Figure 9: Hull/empennage-pitching moment curve

When the angle of attack exceeds a certain range, the tail shows control over the pitching moment. When -18 degrees≤α≤18 degrees, the pitching moment coefficient of double-ellipsoidal airship changes linearly. In this range, airship with X-shaped tail and inverted Y-shaped tail have similar variation trends. When α>18 degrees or α<-18 degrees, the airship inverted Y-shaped tail has a larger pitching moment coefficient than the airship with X-shaped tail. By analyzing the values of the pitching moment generated by the tail wing and the hull of double-ellipsoidal airship respectively, the pitching moment generated by the tail wing is positive and the pitching moment generated by the hull is negative, and the values increase with the increase of the angle of attack. When 0 degrees≤α≤18 degrees, the slope of the pitching moment curve generated by the hull is greater than that generated by the tail wing. When 18 degrees≤α≤30 degrees, the slope of the pitching moment curve generated by the tail wing is greater than that generated by the hull.

4. Analysis of wind load simulation results

Through the simulation of double-ellipsoidal airships with X-shaped tail and inverted Y-shaped tail at different angles of attack and sideslip, the wind load on the hull surface under the set boundary conditions is obtained.

4.1. Lift effect analysis

For double-ellipsoidal airship with X-shaped tail, the simulation results of surface wind load under the condition of angle of attack of 0 degrees, 10 degrees and 20 degrees are shown in the Figure 10, Figure 11 and Figure 12.

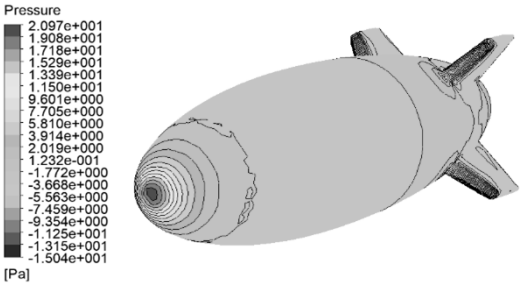

Figure 10: Surface wind pressure at angle of attack 0 degrees

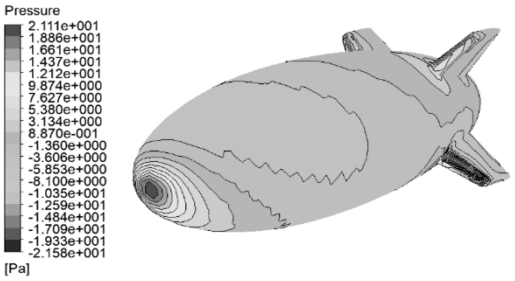

Figure 11: Surface wind pressure at angle of attack 10 degrees

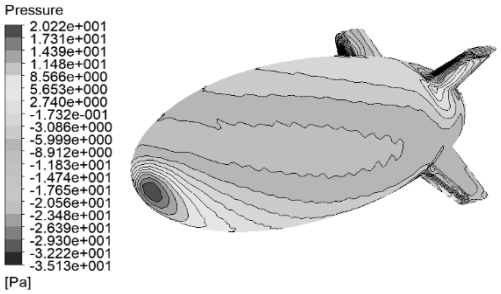

Figure 12: Surface wind pressure at angle of attack 20 degrees

The simulation results show that with the increase of the attack angle of the airship, the positive pressure area at the front end of the airship gradually moves to the bottom of the airship. When the angle of attack is 0 degrees, the wind pressure on the double-ellipsoidal airship surface presents a symmetrical distribution and the value of lift is basically 0. When the angle of attack increases, the upper part of the lower tail of the airship shows negative pressure, the lower part of the upper tail of the airship shows positive pressure. The airship is subjected to upward aerodynamic force.

The surface wind load of double-ellipsoidal airship with inverted Y-shaped tail at the sideslip angle of 5 degrees and 15 degrees are shown in the Figure 13 and Figure 14. The simulation results of surface wind load of airship with X-shaped tail under the condition of sideslip angle of 15 degrees are shown in the Figure 15.

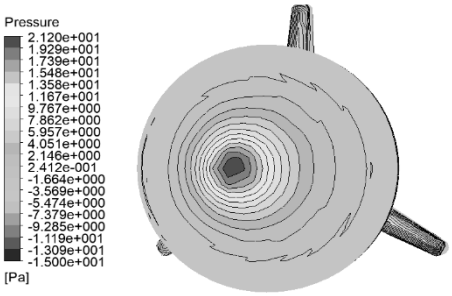

Figure 13: Surface wind pressure at sideslip angle 5 degrees

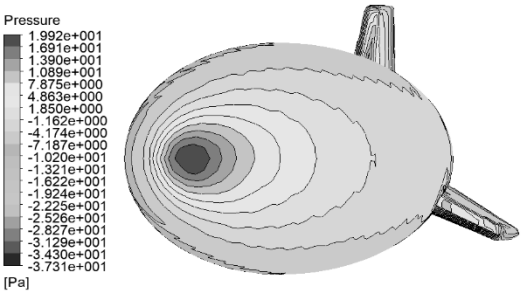

Figure 14: Surface wind pressure at sideslip angle 15 degrees

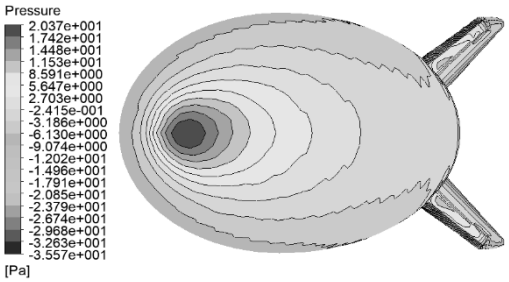

Figure 15: Surface wind pressure at sideslip angle 15 degrees

The simulation results show that with the increase of sideslip angle, positive pressure is generated on the upper side of the lower tail of double-ellipsoidal airship with inverted Y-shaped tail, and negative pressure is generated on the lower side of the lower tail. For double-ellipsoidal airship with X-shaped tail, the wind pressure on the upper and lower tail wing are symmetrically distributed with the change of sideslip angle.

4.2. Pitching moment analysis

The surface wind load simulation is carried out for double-ellipsoidal airship with X-shaped tail with an angle of attack of 0 degrees, 10 degrees, 20 degrees and 30 degrees. The distribution of wind pressure on the upper and lower tail surfaces of the airship is shown in the Figure 16 to Figure 22.

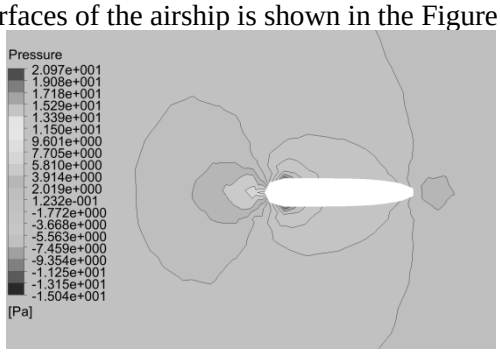

Figure 16: Wind pressure nephogram of tail wing with angle of attack of 0 degrees

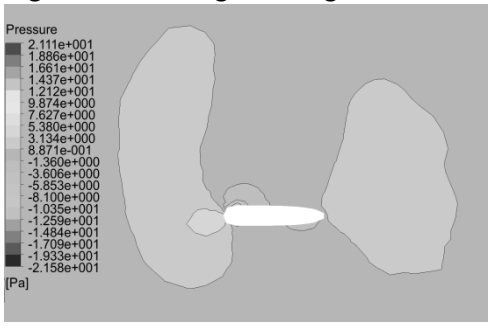

Figure 17: Wind pressure nephogram of upper tail wing with angle of attack of 10 degrees

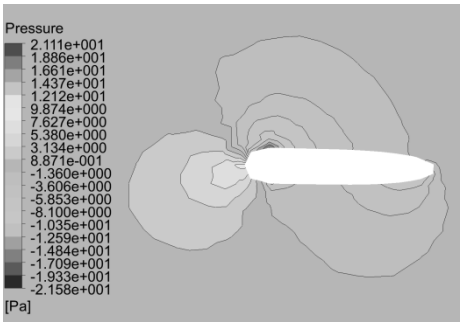

Figure 18: Wind pressure nephogram of lower tail wing with angle of attack of 10 degrees

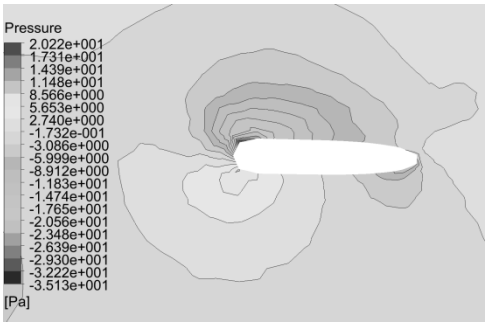

Figure 19: Wind pressure nephogram of upper tail wing with angle of attack of 20 degrees

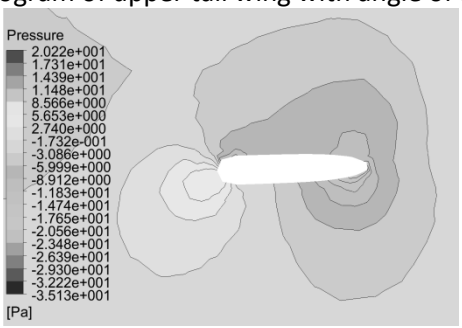

Figure 20: Wind pressure nephogram of lower tail wing with angle of attack of 20 degrees

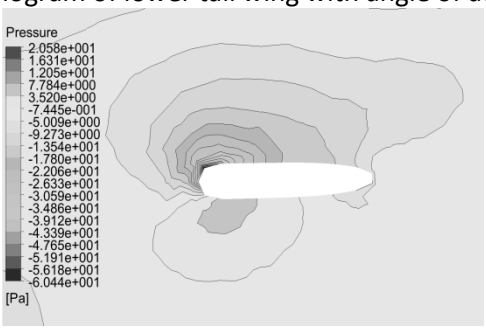

Figure 21: Wind pressure nephogram of upper tail wing with angle of attack of 30 degrees

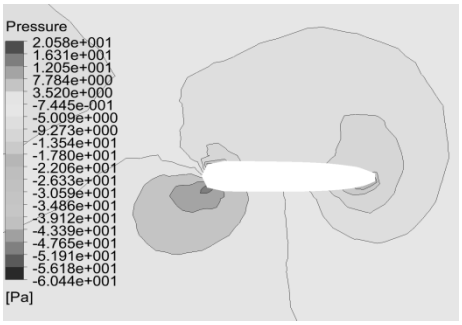

Figure 22: Wind pressure nephogram of lower tail wing with angle of attack of 30 degrees

The simulation results show that when the angle of attack is 0 degrees, the surface wind pressure of the upper and lower tail of double-ellipsoidal airship with X-shaped tail is basically the same, and the pitching moment generated by aerodynamic force is basically 0. With the increase of the angle of attack, the distribution trend of wind pressure on the upper and lower tail surfaces changes. The positive pressure region gradually moves from the front end of the tail to the lower part, and the negative pressure area gradually moves from the upper and lower sides of the tail to the upper part of the front end of the tail and the lower part of the rear end of the tail. The intensity of positive pressure and negative pressure is gradually increasing, which makes the airship subject to positive pitching torque.

5. Conclusions

Compared with double-ellipsoidal airship with X-shaped tail, the airship with inverted Y-shaped tail has certain advantages in reducing hull resistance. Compared with airship with inverted Y-shaped tail, the airship with X-shaped tail has stronger ability to provide lift and maintain hull stability.

From the perspective of flight control, the strategy of flying at a small angle of attack can not only provide a certain lift for the double-ellipsoidal airship, but also maintain its resistance and pitching moment at a low level.

Based on the research results of this paper, the combination research of different wing forms and different hull shapes can be carried out to obtain the optimal combination of aerodynamic characteristics of airship shape.

6. References

[1] G. Xiaofeng，D. Dongbei，G. Xin, Study on the volume design of stratospheric airship capsule and the variation law of net buoyancy. Proceedings of China aerostat Conference (2007) 91–99.

[2] Z. Zhongyu, Numerical investigation on aerodynamic performance of stratosphere airship. Harbin Institute of Technology. 12 (2014) 5-6.

[3] Z. Guifu, Analysis of the influence of tail airfoil on tethered balloon. Science & Technology Vision. 15 (2020) 83-85.

[4] Z. Haijun, G. Xueyan, Y. Fan, Influences of geometry of hull tail on aerodynamic drag of stratospheric airships. Journal of Aerospace Power. 30 (2015) 555-562.

[5] Z. Dan, G. Xueyan, Numerical analyses on ambient flow of a double-axis ellipsoidal stratospheric airship. Chinese Quarterly of Mechanics, 29 (2008) 556-564.

[6] J. Anfan, S. Wenping, Study of Airship Shapes by Calculating Drag Characteristics. Aeronautical Computing Technique. 36 (2006) 100-103.

[7] W. Xiaoliang, Aerodynamic Estimation for Stratosphere Airship. Chinese Quarterly of Mechanics. 27 (2006) 295-304.

[8] L. Ruikun, G. Xueyan, Numerical analysis of aerodynamic performance for stratospheric airship with a propeller. Chinese Quarterly of Mechanics. 31 (2010) 355-362.

[9] L. Tiane, S. Xiaoying, Z. Zhongyu, Numerical simulation and formula fitting of aerodynamic drag force of stratophere airship. Engineering Mechanics. 34 (2017) 249-256.

[10] W. Wang, X. Liu, Aerodynamic characteristics analysis of stratospheric airship configuration. Chinese spacecraft recovery & remote sensing. 28 (2007) 55-61.

[11] Y. Feng, J. Luhua, C. Yanxiang, Aerodynamic Performance Analysis of Layout of Airship Hull. Computer Simulation. 31 (2014) 97-102.

[12] M. Baigang, Calculating Dynamic Derivative and Modeling Nonlinear Unsteady Aerodynamics Based on CFD. Northwestern Polytechnical University. (2018) 23-30.